# Domain Walls Seeding the Electroweak Phase Transition

Simone Blasi* and Alberto Mariotti†
*Theoretische Natuurkunde and IIHE/ELEM, Vrije Universiteit Brussel,
and The International Solvay Institutes, Pleinlaan 2, B-1050 Brussels, Belgium*

(Received 15 June 2022; revised 23 September 2022; accepted 21 November 2022; published 23 December 2022)

Topological defects can act as local impurities that seed cosmological phase transitions. In this Letter, we study the case of domain walls and how they can affect the electroweak phase transition in the singlet-extended standard model with a $Z_2$-symmetric potential. When the transition occurs in two steps, the early breaking of the $Z_2$ symmetry implies the formation of domain walls which then act as nucleation sites for the second step. We develop a method based on a Kaluza-Klein decomposition to calculate the rate of the catalyzed phase transition within the 3D theory on the domain wall surface. By comparison with the standard homogeneous rate, we conclude that the seeded phase transition is generically faster and it ultimately determines the way the phase transition is completed. We finally comment on the phenomenological implications for gravitational waves.

DOI: 10.1103/PhysRevLett.129.261303

*Introduction.*—Cosmological phase transitions are of primary importance in high energy physics as they can shed light on major open questions in the standard model (SM), such as the matter-antimatter asymmetry in the Universe, and the dynamics of electroweak symmetry breaking thanks to the exciting prospects for detecting the corresponding background of gravitational waves (GWs), see, e.g., [1,2].

In the case of first order transitions, their physics crucially depends on the mechanism controlling the nucleation of bubbles, which is commonly assumed to proceed via thermal or quantum fluctuations in homogeneous spacetime.

However, the presence of impurities at the time of the transition can catalyze bubble nucleation, thus providing a competing mechanism for the decay of the false vacuum [3–7]. Following [3], we will refer to this case as inhomogeneous or seeded nucleation, as the tunneling probability is not uniformly distributed on the spacetime but it is enhanced at the location of the seeds.

The nature of the impurities can be vastly different, including black holes [8–15], local overdensities [16–18], and temperature fluctuations [19], as well as topological defects [3–5,7,20–31] for which most studies have focused on cosmic strings [5,21–27] and monopoles [3,4,28–30].

In this Letter, we will consider the case of domain walls (DWs) (see Refs. [32,33] for related work in $1+1$ dimensions), two-dimensional defects related to the spontaneous breakdown of a discrete symmetry [34,35], for which we provide a coherent thermal history from the time of formation to the subsequently induced seeded phase transition in the early Universe.

In order to study the seeded nucleation, we introduce a new method based on a Kaluza-Klein (KK) decomposition along the direction orthogonal to the walls. This circumvents the task of solving a nontrivial system of partial differential equations, and at the same time gives a more physical picture of the inhomogeneous tunneling as a lower-dimensional homogeneous transition.

Even though this formalism is rather general, our case of study will be the electroweak phase transition within one of the simplest and most popular extensions of the SM, the XSM, see e.g., [36–62], where the only new particle is a real scalar field $S$, singlet under the SM gauge group, and odd under a $Z_2$ symmetry.

We will show the existence of a new type of electroweak phase transition in the XSM that is catalyzed by the DWs formed when the singlet scalar develops a vacuum expectation value (VEV). Bubbles of true vacuum will be nucleated inside the DWs and expand, eventually collapsing the wall network. This process will be faster than the homogeneous nucleation, and therefore it will be the one responsible for completing the transition with important phenomenological implications.

*Setup and nucleation condition.*—Our case of study is the SM extended with a real scalar singlet $S$, odd under a $Z_2$ symmetry $S \to -S$. The renormalizable potential in the unitary gauge reads

$$V(h,S) = -\frac{\mu^2}{2}h^2 + \frac{\lambda}{4}h^4 - \frac{m^2}{2}S^2 + \frac{\eta}{4}S^4 + \frac{\kappa}{2}h^2S^2, \qquad (1)$$

and we take the parameters $\mu^2$, $m^2$, $\eta$ as well as the "portal coupling" with the Higgs $\kappa$ to be positive. The physical singlet mass in the zero-temperature vacuum ($h = v$, $S = 0$) is $m_S^2 \equiv \kappa v^2 - m^2$, with $v = 246$ GeV.

Throughout this Letter, we will perform a perturbative study of the electroweak phase transition (see, e.g., [63–68] for nonperturbative approaches to this subject), and we will account for temperature corrections by retaining the leading order in the high-temperature approximation. This amounts to work with thermal masses given by

$$\mu^2(T) = \mu^2 - c_h T^2, \qquad m^2(T) = m^2 - c_s T^2, \quad (2)$$

where $c_h$ and $c_s$ read [43]

$$c_h = \frac{2m_W^2 + m_Z^2 + m_h^2 + 2m_t^2}{4v^2} + \frac{\kappa}{12}, \quad c_s = \frac{4\kappa + 3\eta}{12}. \quad (3)$$

Our focus is a two-step electroweak phase transition in which at high temperatures all symmetries are restored. The first step entails the spontaneous breaking of the $Z_2$ symmetry at the temperature $T_d$, with the singlet scalar developing a nonzero VEV, $v_s(T) = m(T)/\sqrt{\eta}$, while the Higgs minimum is still at zero. Given that the two vacua $\langle S \rangle = \pm v_s(T)$ are energetically equivalent, regions with $+$ and $-$ will form inside a Hubble patch separated by DWs with profile

$$S_{\rm DW}(z) = v_s(T)\tanh[m(T)z/\sqrt{2}], \quad (4)$$

and tension given by $\sigma_{\rm DW} = \sqrt{8\eta}v_s(T)^3/3$, see, e.g., [69].

At temperatures below the critical temperature $T_c$, the $(0, \pm v_s)$ vacua become metastable and decay to the (true) electroweak vacuum $(v, 0)$. This second and last step is usually assumed to occur in homogeneous spacetime, equivalently either inside the $+$ or $-$ domains, and it is typically first order owing to the nonzero singlet VEV. The whole process may then be summarized as

$$(0,0) \to (0, v_s) \to (v, 0). \quad (5)$$

The presence of the DWs can, however, induce a seeded vacuum decay which can only happen close to the boundary between the $+/-$ domains, thus providing a competing mechanism for the second step in (5) (homogeneous tunneling can in fact still occur far from the DWs).

In order to quantitatively describe the tunneling catalyzed by the DWs, it is natural to define a nucleation rate per unit surface given by [20,23]

$$\gamma_S \equiv \frac{\Gamma}{S} = A' \exp(-S_{\rm inh}), \quad (6)$$

where $A' \sim \sigma_{\rm DW}$ and $S_{\rm inh}$ is the action describing the inhomogeneous tunneling. In order to find the nucleation condition in the expanding Universe, we parametrize the total surface occupied by the DWs inside one Hubble volume as $S_H = \xi H^{-2}$, where $\xi$ is $\mathcal{O}(1)$ in the scaling regime [69]. The condition defining the nucleation temperature $T_n$ is then

$$\mathcal{N}(T_n) \equiv \int_{T_n}^{T_c} \xi \frac{\gamma_S}{H^3} \frac{dT}{T} = 1. \quad (7)$$

In a radiation-dominated Universe we obtain

$$S_{\rm inh} \simeq 3 \log \frac{M_{\rm Pl}}{T_n} + \log \frac{\sigma_{\rm DW}}{T_n^3} + \log \xi - 8.5 \approx 105, \quad (8)$$

where we have taken the DW tension and the nucleation temperature to be at the electroweak scale.

The action $S_{\rm inh}$ is associated with the formation of a bubble that modifies the original DW profile due to the onset of a nonzero Higgs VEV at its core, and will be evaluated with the methods discussed in the next section.

*Seeded phase transition.*—The starting point for our formalism is the following ansatz for the fields in the background of the unperturbed DW in the spirit of a KK decomposition,

$$S = S_{\rm DW}(z) + \sum_k s_k(x)\sigma_k(z), \quad h = \sum_k h_k(x)\phi_k(z). \quad (9)$$

The sum runs over a complete set of profiles, $\sigma_k(z)$ and $\phi_k(z)$, which are chosen such that the quadratic part of the 3D action, obtained after integration over the $z$ direction orthogonal to the DW, is canonical and diagonal (the 3D theory we will refer to should not be confused with the dimensionally reduced theory for the light Matsubara modes at finite temperature),

$$\mathcal{S}^{(2)} = \int d^3x \left[\frac{1}{2}(\partial_\mu h_k)^2 + \frac{1}{2}(\partial_\mu s_k)^2 - \frac{\omega_k^2}{2}h_k^2 - \frac{m_k^2}{2}s_k^2\right].$$

The 3D masses $\omega_k^2$ and $m_k^2$ are understood as the spectrum of bound and scattering states for a Pösch-Teller potential $\propto S_{\rm DW}^2$ in quantum mechanics, and can be found exactly with the corresponding eigenfunctions $\sigma_k$ and $\phi_k$, see, e.g., [70,71]. Neglecting the massless mode due to the breaking of translational invariance in (9), the singlet modes consist of a unique bound state $s_0$, with mass $m_0^2 = 3/2m^2(T)$, and a gapped continuum starting at $m_{\rm KK}^2 = 2m^2(T)$. As $m^2(T) > 0$ for temperatures below the $Z_2$ spontaneous breaking all these states have positive-definite masses.

The Higgs spectrum is qualitatively the same, with the difference that more bound states are possibly allowed depending on the ratio $\kappa/\eta$, and that their masses can be of either sign. In the parameter space of interest there will be a single Higgs bound state $h_0$ with mass

$$\omega_0^2 = \frac{1}{2} p m^2(T) - \mu^2(T), \quad (10)$$

where $p(p+1)/2 \equiv \kappa/\eta$. The gapped Higgs continuum similarly starts at $\omega_{\rm KK}^2 = (\kappa/\eta) m^2(T) - \mu^2(T)$.

In order to make the problem tractable, we will take advantage of the mass gap between the discrete states $(h_0, s_0)$ and the continuum scattering states by integrating out the latter at tree level (see Ref. [71] for more details). The resulting EFT consists of $s_0$ and $h_0$ as the only dynamical modes. Their interactions are inherited from the 4D potential in (1) as well as mediated by the tree-level exchange of the continuum modes, and can be described by an effective potential $V_{\rm eff}^{\rm 3D}$ given by

$$\begin{aligned} V_{\rm eff}^{\rm 3D} = &\frac{1}{2}\omega_0^2 h_0^2 + \frac{1}{2} m_0^2 s_0^2 \\ &+ c_{3\eta} m^{3/2}\sqrt{\eta} s_0^3 + c_{3\kappa} m^{3/2}\frac{\kappa}{\sqrt{\eta}} s_0 h_0^2 \\ &+ \frac{1}{4}(c_\lambda m)\lambda h_0^4 + \frac{1}{2}(c_{4\kappa} m)\kappa h_0^2 s_0^2 + \frac{1}{4}(c_{4\eta} m)\eta s_0^4 \\ &+ \frac{1}{m_{\rm KK}^2} P_6(h_0, s_0) + \frac{1}{m_{\rm KK}^4} P_8(h_0, s_0), \end{aligned} \quad (11)$$

where the $c$ coefficients are $\lesssim \mathcal{O}(1)$ numbers, and we have dropped the explicit temperature dependence on the parameters. The effective interactions mediated by the continuum states are displayed in the last line of (11), where $P_{6,8}$ are polynomials in $h_0$ and $s_0$ of sixth and eighth order, respectively, and $m_{\rm KK}$ indicates the generic scale of the continuum masses.

The key advantage of this approach is that the DW dynamics and the seeded phase transitions can now be understood in terms of the 3D effective potential in (11). According to our ansatz in (9), the initial DW configuration corresponds to all the 3D modes set to zero, which effectively means $h_0 = s_0 = 0$ in the EFT. Since $m_0^2$ is positive definite, we need to consider only the lightest Higgs mode: when $\omega_0^2 > 0$ the DW configuration is either a local or global minimum of the theory, whereas $\omega_0^2 < 0$ implies a runaway direction and the DW is classically unstable.

Let us first consider the case in which $\omega_0^2 > 0$ for all temperatures. For $T > T_c$ the DW configuration is stable and the 3D minimum with $(h_0 = 0, s_0 = 0)$ is global. On the other hand for $T < T_c$ the DW configuration is metastable, since in the 4D theory the global minimum is now $S = 0$ and $h \neq 0$, and correspondingly the 3D minimum can only be local. The seeded phase transition can then be described in terms of (11) as the decay of the metastable vacuum $(h_0 = 0, s_0 = 0)$:

$$(0,0)_{\rm 3D} \to (\langle h_0\rangle, \langle s_0\rangle)_{\rm 3D}, \quad (12)$$

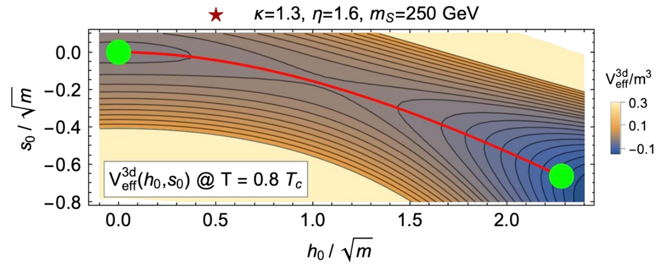


FIG. 1. Contours for the effective potential (11) in the $(h_0, s_0)$ plane, and O(2) tunneling trajectory (solid red line) obtained with COSMOTRANSITIONS for the choice of the parameters $\kappa$, $\eta$, $m_S$ as indicated in the figure, evaluated at $T = 0.8T_c$, with $T_c \simeq 110$ GeV. The initial DW configuration corresponds to the metastable vacuum $h_0 = s_0 = 0$.

where $\langle\cdots\rangle$ denotes the generic release point, which needs to lie within the EFT validity for consistency. The transition above is guaranteed to be first order due to the positive $h_0$ and $s_0$ masses.

This transition is homogeneous in the 3D theory and corresponds to O(2) symmetric bubbles nucleated on the DW plane, which are time independent in the high-temperature limit. The nucleation rate can be obtained with standard techniques, e.g., with COSMOTRANSITIONS [74] [neglecting derivative operators arising at $\mathcal{O}(1/m_{\rm KK}^4)$]. The corresponding bounce action will be indicated by $S_{\rm inh} = S_2/T$. An example of tunneling trajectory is shown in Fig. 1 for a particular choice of model parameters.

Let us now comment on the case in which $\omega_0^2$ turns negative at some temperature $T_r$ such that $\omega_0^2(T_r) = 0$. The case in which $T_r < T_c$ is actually described by seeded tunneling as explained above: as $\omega_0^2$ goes to zero for $T \to T_r$ the barrier around $(0,0)_{\rm 3D}$ becomes smaller and smaller, ensuring successful nucleation for some temperature between $T_r$ and $T_c$.

The case in which $\omega_0^2$ turns negative for $T_r > T_c$ is not generic in the model parameter space and will not be discussed here.

The rate of seeded tunneling can also be evaluated by employing the thin wall approximation. This amounts to approximate the energy difference between the false vacuum and the bounce configuration $\Delta E$ in terms of key quantities such as the size of the bubble $R$, its tension $\sigma_B$ (see Ref. [71] for a discussion on how to estimate the bubble tension in a multifield potential in the thin wall limit), and the energy difference between the false and true vacuum, $\epsilon$.

When the transition is seeded by a DW, however, one has to take into account that part of the DW surface will be eaten in the process of nucleation. This leads to the following estimate:

$$\Delta E(R) = 4\pi R^2 \sigma_B - \frac{4}{3}\pi R^3 \epsilon - \pi R^2 \sigma_{\rm DW}, \quad (13)$$

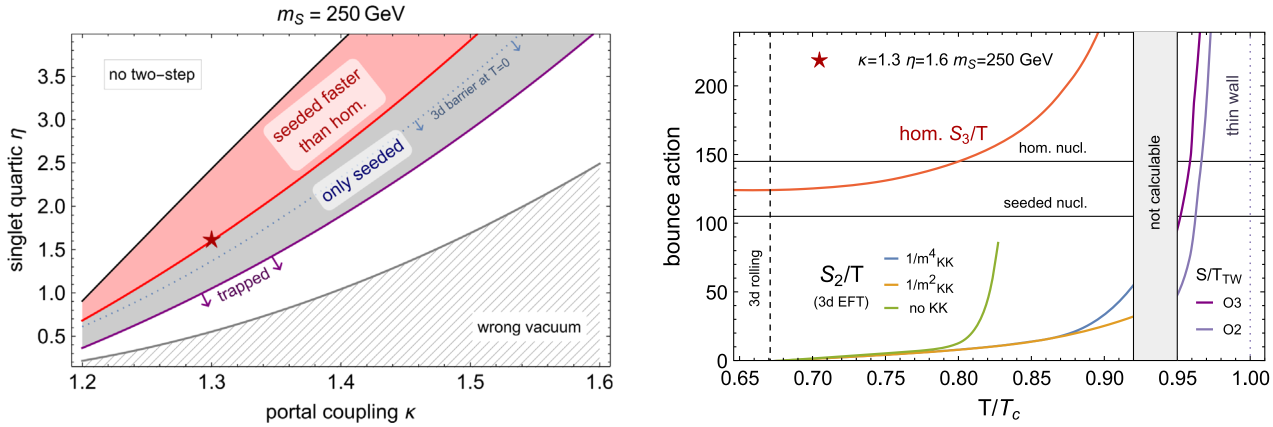


FIG. 2. Left: scan in the $(\kappa, \eta)$ parameter space for $m_S = 250$ GeV. In the upper left corner the phase transition does not follow the two-step process of (5), whereas in the bottom right corner the $T = 0$ vacuum is not the electroweak one. In the red region the seeded nucleation is faster than the homogeneous one, whereas in the blue region homogeneous bubbles fail to nucleate, but seeded bubbles can complete the phase transition. Below the purple line the system remains trapped in the false vacuum. Right: comparison of the bounce action for the homogeneous tunneling $S_3/T$, and for the seeded tunneling $S_2/T$ (with different approximations in the EFT) and $S/T_{\rm TW}$ in the thin wall limit, as a function of the temperature for $m_S = 250$ GeV, $\kappa = 1.3$, and $\eta = 1.6$.

where we have assumed that the nucleated bubble is approximately spherical. Maximizing the energy we obtain the size of the critical bubble $R_*$ and the corresponding action

$$S_{\rm inh} \approx \frac{\Delta E(R_*)}{T} = \frac{16\pi(\sigma_B - \sigma_{\rm DW}/4)^3}{3T\epsilon^2}. \quad (14)$$

A more refined ansatz can be made to account for deviations from spherical symmetry, as for instance considering an O(2) symmetric ellipsoid centered on the DW (see Ref. [71] for details), which gives qualitatively similar results.

For $\sigma_{\rm DW} \to 0$, Eq. (14) clearly coincides with the transition rate in homogeneous spacetime [75–77]. On the other hand, the presence of a DW with nonzero tension always reduces the barrier and thus catalyzes the transition.

*Results and conclusion.*—An overview of our results is shown in the left panel of Fig. 2 as a scan over the model parameter space fixing the singlet mass to a representative value. Because of the presence of the DWs, seeded vacuum decay always occurs before the would-be homogeneous nucleation in all the two-step parameter space. In the red region, homogeneous nucleation is possible but seeded nucleation is faster. This is determined for each point by identifying the would-be homogeneous nucleation temperature, and evaluating the action $S_2/T$ within the 3D effective potential (11) at this temperature. As this turns out to be below the nucleation condition, we conclude that seeded nucleation must have occurred before the homogeneous one.

Outside the red region homogeneous bubbles fail to nucleate and the transition can only complete by seeded tunneling, opening up the new viable parameter space colored in blue, which is determined by requiring successful nucleation at some temperature in the EFT. The dotted blue line indicates the parameter space where $\omega_0^2$ remains positive at $T = 0$, meaning that the barrier in $V_{\rm eff}^{\rm 3D}$ will never vanish and fields may remain stuck in the false vacuum depending on the nucleation rate. This is in fact the case for points below the purple line where even seeded bubbles fail to nucleate.

The interplay of homogeneous and seeded nucleation is shown in detail in the right panel of Fig. 2 for the benchmark point indicated by the red star in the left panel. The red line shows the standard $S_3/T$ action for the homogeneous tunneling, for which the nucleation condition is fulfilled at $T \sim 0.8T_c$, with $T_c = 110$ GeV. This benchmark predicts a (would-be) classical instability of the DWs around $T_r \sim 0.65T_c$ where $\omega_0^2$ vanishes.

The $S_2/T$ action is evaluated according to various levels of approximation within the effective 3D potential, namely neglecting altogether the contribution from the continuum states, corresponding to neglecting the last line in (11) (green line); at the order $\mathcal{O}(1/m_{\rm KK}^2)$ and thus neglecting $P_8$ in (11) (orange line); at $\mathcal{O}(1/m_{\rm KK}^4)$ including all the terms in (11) (blue line). Close to $T_r$ all the approximations predict the same value of $S_2/T$ because the barrier is small and the release point is very close to the origin, while at higher temperatures they start differing. This is understood by noticing that close to $T_c$ the false and true vacuum become almost degenerate, and the critical bubble will have a larger volume for the energy gain to balance its tension. Within the 3D theory this means that the bulk effects from the direction orthogonal to the DW, which are controlled by the continuum states, become increasingly important making this region hardly tractable in the EFT.

Very close to $T_c$, however, the bubble is expected to become thin and the approximation (14) to work reliably. The prediction for the seeded bounce action in the thin wall approximation $S/T_{\rm TW}$, is shown in the right panel of Fig. 2 by the purple and light-purple line for a spherical ansatz $O(3)$, and for an ellipsoid with O(2) symmetry (which gives the least action), respectively. The corresponding nucleation temperature according to (8) is estimated to be $\sim 0.97 T_c$. We also indicate a small gap of calculability where our methods suffer from theoretical uncertainty, namely extrapolation of the thin wall away from $T_c$ and significantly different results for the $\mathcal{O}(1/m_{\rm KK}^2)$ and $\mathcal{O}(1/m_{\rm KK}^4)$ predictions.

The GW signal associated to this new type of phase transition is yet to be explored. Nonetheless, we can expect it to differ from its homogeneous counterpart due to (i) a large violation of spherical symmetry of the bubbles (see Ref. [71] for the detailed shape), and (ii) the effective duration of the transition is here set by the average distance among the defects [7] rather than the slope of the free energy, meaning that for $\xi \sim \mathcal{O}(1)$ the GW signal can be naturally amplified. In addition, (iii) the presence of different physical scales (average distance between bubbles nucleated on the same wall, and wall-wall distance) may result in characteristic spectral features that can be searched for in the upcoming GW data.

We are grateful to Riccardo Argurio and Diego Redigolo for useful discussions and comments on the draft. We also thank Luigi Tizzano and Iason Baldes for useful discussions. S. B. and A. M. are supported by the Strategic Research Program High-Energy Physics and the Research Council of the Vrije Universiteit Brussel, and by the “Excellence of Science–EOS”—be.h Project No. 30820817.

[*]simone.blasi@vub.be
[†]alberto.mariotti@vub.be

[1] E. Barausse *et al.*, Prospects for fundamental physics with LISA, Gen. Relativ. Gravit. **52**, 81 (2020).
[2] R. Caldwell *et al.*, Detection of early-Universe gravitational wave signatures and fundamental physics, in *2022 Snowmass Summer Study* (2022), arXiv:2203.07972.
[3] P. J. Steinhardt, Monopole and vortex dissociation and decay of the false vacuum, Nucl. Phys. **B190**, 583 (1981).
[4] P. J. Steinhardt, Monopole dissociation in the early Universe, Phys. Rev. D **24**, 842 (1981).
[5] L. G. Jensen and P. J. Steinhardt, Dissociation of Abrikosov-Nielsen-Olesen vortices, Phys. Rev. B **27**, 5549 (1983).
[6] Y. Hosotani, Impurities in the early Universe, Phys. Rev. D **27**, 789 (1983).
[7] E. Witten, Cosmic separation of phases, Phys. Rev. D **30**, 272 (1984).
[8] W. A. Hiscock, Can black holes nucleate vacuum phase transitions?, Phys. Rev. D **35**, 1161 (1987).
[9] D. R. Green, E. Silverstein, and D. Starr, Attractor explosions and catalyzed vacuum decay, Phys. Rev. D **74**, 024004 (2006).
[10] R. Gregory, I. G. Moss, and B. Withers, Black holes as bubble nucleation sites, J. High Energy Phys. 03 (2014) 081.
[11] P. Burda, R. Gregory, and I. Moss, Vacuum metastability with black holes, J. High Energy Phys. 08 (2015) 114.
[12] K. Mukaida and M. Yamada, False vacuum decay catalyzed by black holes, Phys. Rev. D **96**, 103514 (2017).
[13] D. Canko, I. Gialamas, G. Jelic-Cizmek, A. Riotto, and N. Tetradis, On the catalysis of the electroweak vacuum decay by black holes at high temperature, Eur. Phys. J. C **78**, 328 (2018).
[14] D.-C. Dai, R. Gregory, and D. Stojkovic, Connecting the Higgs potential and primordial black holes, Phys. Rev. D **101**, 125012 (2020).
[15] B. K. El-Menoufi, S. J. Huber, and J. P. Manuel, Black holes seeding cosmological phase transitions, arXiv:2006.16275.
[16] N. Oshita, M. Yamada, and M. Yamaguchi, Compact objects as the catalysts for vacuum decays, Phys. Lett. B **791**, 149 (2019).
[17] R. Balkin, J. Serra, K. Springmann, S. Stelzl, and A. Weiler, Density induced vacuum instability, arXiv:2105.13354.
[18] D.-C. Dai, D. Minic, and D. Stojkovic, Interaction of cosmological domain walls with large classical objects, like planets and satellites, and the flyby anomaly, J. High Energy Phys. 03 (2022) 207.
[19] R. Jinno, T. Konstandin, H. Rubira, and J. van de Vis, Effect of density fluctuations on gravitational wave production in first-order phase transitions, J. Cosmol. Astropart. Phys. 12 (2021) 019.
[20] J. Preskill and A. Vilenkin, Decay of metastable topological defects, Phys. Rev. D **47**, 2324 (1993).
[21] U. A. Yajnik, Phase transition induced by cosmic strings, Phys. Rev. D **34**, 1237 (1986).
[22] U. A. Yajnik and T. Padmanabhan, Analytical approach to string induced phase transition, Phys. Rev. D **35**, 3100 (1987).
[23] I. Dasgupta, Vacuum tunneling by cosmic strings, Nucl. Phys. **B506**, 421 (1997).
[24] B. Kumar and U. A. Yajnik, On stability of false vacuum in supersymmetric theories with cosmic strings, Phys. Rev. D **79**, 065001 (2009).
[25] B.-H. Lee, W. Lee, R. MacKenzie, M. B. Paranjape, U. A. Yajnik, and D.-h. Yeom, Battle of the bulge: Decay of the thin, false cosmic string, Phys. Rev. D **88**, 105008 (2013).
[26] B.-H. Lee, W. Lee, R. MacKenzie, M. B. Paranjape, U. A. Yajnik, and D.-h. Yeom, Tunneling decay of false vortices, Phys. Rev. D **88**, 085031 (2013).
[27] I. Koga, S. Kuroyanagi, and Y. Ookouchi, Instability of Higgs vacuum via string cloud, Phys. Lett. B **800**, 135093 (2020).
[28] B. Kumar and U. Yajnik, Graceful exit via monopoles in a theory with O’Raifeartaigh type supersymmetry breaking, Nucl. Phys. **B831**, 162 (2010).
[29] B. Kumar, M. B. Paranjape, and U. A. Yajnik, Fate of the false monopoles: Induced vacuum decay, Phys. Rev. D **82**, 025022 (2010).
[30] P. Agrawal and M. Nee, The boring monopole, SciPost Phys. **13**, 049 (2022).

[31] D. I. Dunsky, A. Ghoshal, H. Murayama, Y. Sakakihara, and G. White, Gravitational wave gastronomy, arXiv:2111.08750.

[32] M. Haberichter, R. MacKenzie, M. B. Paranjape, and Y. Ung, Tunneling decay of false domain walls: the silence of the lambs, J. Math. Phys. (N.Y.) **57**, 042303 (2016).

[33] E. Dupuis, Y. Gobeil, R. MacKenzie, L. Marleau, M. B. Paranjape, and Y. Ung, Tunneling decay of false kinks, Phys. Rev. D **92**, 025031 (2015).

[34] Y. B. Zeldovich, I. Y. Kobzarev, and L. B. Okun, Cosmological consequences of the spontaneous breakdown of discrete symmetry, Zh. Eksp. Teor. Fiz. **67**, 3 (1974).

[35] T. W. B. Kibble, Topology of cosmic domains and strings, J. Phys. A **9**, 1387 (1976).

[36] J. McDonald, Gauge singlet scalars as cold dark matter, Phys. Rev. D **50**, 3637 (1994).

[37] C. P. Burgess, M. Pospelov, and T. ter Veldhuis, The minimal model of nonbaryonic dark matter: A Singlet scalar, Nucl. Phys. **B619**, 709 (2001).

[38] S. J. Huber and M. G. Schmidt, Electroweak baryogenesis: Concrete in a SUSY model with a gauge singlet, Nucl. Phys. **B606**, 183 (2001).

[39] J. R. Espinosa and M. Quiros, Novel effects in electroweak breaking from a hidden sector, Phys. Rev. D **76**, 076004 (2007).

[40] S. Profumo, M. J. Ramsey-Musolf, and G. Shaughnessy, Singlet Higgs phenomenology and the electroweak phase transition, J. High Energy Phys. 08 (2007) 010.

[41] V. Barger, P. Langacker, M. McCaskey, M. J. Ramsey-Musolf, and G. Shaughnessy, LHC phenomenology of an extended standard model with a real scalar singlet, Phys. Rev. D **77**, 035005 (2008).

[42] J. R. Espinosa, T. Konstandin, J. M. No, and M. Quiros, Some cosmological implications of hidden sectors, Phys. Rev. D **78**, 123528 (2008).

[43] J. R. Espinosa, T. Konstandin, and F. Riva, Strong electroweak phase transitions in the standard model with a singlet, Nucl. Phys. **B854**, 592 (2012).

[44] J. M. Cline and K. Kainulainen, Electroweak baryogenesis and dark matter from a singlet Higgs, J. Cosmol. Astropart. Phys. 01 (2013) 012.

[45] P. H. Damgaard, D. O'Connell, T. C. Petersen, and A. Tranberg, Constraints on New Physics from Baryogenesis and Large Hadron Collider Data, Phys. Rev. Lett. **111**, 221804 (2013).

[46] S. Profumo, M. J. Ramsey-Musolf, C. L. Wainwright, and P. Winslow, Singlet-catalyzed electroweak phase transitions and precision Higgs boson studies, Phys. Rev. D **91**, 035018 (2015).

[47] L. Feng, S. Profumo, and L. Ubaldi, Closing in on singlet scalar dark matter: LUX, invisible Higgs decays and gamma-ray lines, J. High Energy Phys. 03 (2015) 045.

[48] D. Curtin, P. Meade, and C.-T. Yu, Testing electroweak baryogenesis with future colliders, J. High Energy Phys. 11 (2014) 127.

[49] N. Craig, H. K. Lou, M. McCullough, and A. Thalapillil, The Higgs portal above threshold, J. High Energy Phys. 02 (2016) 127.

[50] J. Kozaczuk, Bubble expansion and the viability of singlet-driven electroweak baryogenesis, J. High Energy Phys. 10 (2015) 135.

[51] P. Huang, A. J. Long, and L.-T. Wang, Probing the electroweak phase transition with Higgs factories and gravitational waves, Phys. Rev. D **94**, 075008 (2016).

[52] V. Vaskonen, Electroweak baryogenesis and gravitational waves from a real scalar singlet, Phys. Rev. D **95**, 123515 (2017).

[53] D. Curtin, P. Meade, and H. Ramani, Thermal resummation and phase transitions, Eur. Phys. J. C **78**, 787 (2018).

[54] G. Kurup and M. Perelstein, Dynamics of electroweak phase transition in singlet-scalar extension of the standard model, Phys. Rev. D **96**, 015036 (2017).

[55] D. Buttazzo, D. Redigolo, F. Sala, and A. Tesi, Fusing vectors into scalars at high energy lepton colliders, J. High Energy Phys. 11 (2018) 144.

[56] K. Ghorbani and P. H. Ghorbani, Strongly first-order phase transition in real singlet scalar dark matter model, J. Phys. G **47**, 015201 (2020).

[57] C. Caprini *et al.*, Detecting gravitational waves from cosmological phase transitions with LISA: An update, J. Cosmol. Astropart. Phys. 03 (2020) 024.

[58] T. Alanne, T. Hugle, M. Platscher, and K. Schmitz, A fresh look at the gravitational-wave signal from cosmological phase transitions, J. High Energy Phys. 03 (2020) 004.

[59] M. Ruhdorfer, E. Salvioni, and A. Weiler, A global view of the off-shell Higgs portal, SciPost Phys. **8**, 027 (2020).

[60] A. Costantini, F. De Lillo, F. Maltoni, L. Mantani, O. Mattelaer, R. Ruiz, and X. Zhao, Vector boson fusion at multi-TeV muon colliders, J. High Energy Phys. 09 (2020) 080.

[61] P. Ghorbani, Vacuum structure and electroweak phase transition in singlet scalar dark matter, Phys. Dark Universe **33**, 100861 (2021).

[62] H. Al Ali *et al.*, The Muon Smasher's guide, Rep. Prog. Phys. **85**, 084201 (2022).

[63] G. D. Moore and K. Rummukainen, Electroweak bubble nucleation, nonperturbatively, Phys. Rev. D **63**, 045002 (2001).

[64] T. Brauner, T. V. I. Tenkanen, A. Tranberg, A. Vuorinen, and D. J. Weir, Dimensional reduction of the standard model coupled to a new singlet scalar field, J. High Energy Phys. 03 (2017) 007.

[65] J. O. Andersen, T. Gorda, A. Helset, L. Niemi, T. V. I. Tenkanen, A. Tranberg, A. Vuorinen, and D. J. Weir, Nonperturbative Analysis of the Electroweak Phase Transition in the Two Higgs Doublet Model, Phys. Rev. Lett. **121**, 191802 (2018).

[66] O. Gould, J. Kozaczuk, L. Niemi, M. J. Ramsey-Musolf, T. V. I. Tenkanen, and D. J. Weir, Nonperturbative analysis of the gravitational waves from a first-order electroweak phase transition, Phys. Rev. D **100**, 115024 (2019).

[67] L. Niemi, M. J. Ramsey-Musolf, T. V. I. Tenkanen, and D. J. Weir, Thermodynamics of a Two-Step Electroweak Phase Transition, Phys. Rev. Lett. **126**, 171802 (2021).

[68] O. Gould, S. Güyer, and K. Rummukainen, First-order electroweak phase transitions: A nonperturbative update, arXiv:2205.07238 [Phys. Rev. D (to be published)].

[69] A. Vilenkin and E. P. S. Shellard, *Cosmic Strings and Other Topological Defects* (Cambridge University Press, Cambridge, England, 2000).

[70] R. Rajaraman, *Solitons and Instantons: An Introduction to Solitons and Instantons in Quantum Field Theory* (North-Holland Publishing Company, 1982).

[71] See Supplemental Material at http://link.aps.org/supplemental/10.1103/PhysRevLett.129.261303 for an extended discussion, which includes Refs. [72,73].

[72] J. McDonald, Cosmological domain wall evolution and spontaneous *CP* violation from a gauge singlet scalar sector, Phys. Lett. B **357**, 19 (1995).

[73] J. R. Espinosa, B. Gripaios, T. Konstandin, and F. Riva, Electroweak baryogenesis in non-minimal composite Higgs models, J. Cosmol. Astropart. Phys. 01 (2012) 012.

[74] C. L. Wainwright, CosmoTransitions: Computing cosmological phase transition temperatures and bubble profiles with multiple fields, Comput. Phys. Commun. **183**, 2006 (2012).

[75] S. R. Coleman, The fate of the false vacuum. 1. Semiclassical theory, Phys. Rev. D **15**, 2929 (1977); **16**, 1248(E) (1977).

[76] A. D. Linde, Decay of the false vacuum at finite temperature, Nucl. Phys. **B216**, 421 (1983); **B223**, 544(E) (1983).

[77] G. W. Anderson and L. J. Hall, The electroweak phase transition and baryogenesis, Phys. Rev. D **45**, 2685 (1992).